

# Asymmetric Flexible Supercapacitor Stack

A. Leela Mohana Reddy · F. Estaline Amitha ·  
Imran Jafri · S. Ramaprabhu

Received: 26 November 2007 / Accepted: 26 March 2008 / Published online: 9 April 2008  
© to the authors 2008

**Abstract** Electrical double layer supercapacitor is very significant in the field of electrical energy storage which can be the solution for the current revolution in the electronic devices like mobile phones, camera flashes which needs flexible and miniaturized energy storage device with all non-aqueous components. The multiwalled carbon nanotubes (MWNTs) have been synthesized by catalytic chemical vapor deposition technique over hydrogen decrepitated Mischmetal (Mm) based  $AB_3$  alloy hydride. The polymer dispersed MWNTs have been obtained by insitu polymerization and the metal oxide/MWNTs were synthesized by sol-gel method. Morphological characterizations of polymer dispersed MWNTs have been carried out using scanning electron microscopy (SEM), transmission electron microscopy (TEM and HRTEM). An assymetric double supercapacitor stack has been fabricated using polymer/MWNTs and metal oxide/MWNTs coated over flexible carbon fabric as electrodes and nafion<sup>®</sup> membrane as a solid electrolyte. Electrochemical performance of the supercapacitor stack has been investigated using cyclic voltammetry, galvanostatic charge-discharge, and electrochemical impedance spectroscopy.

**Keywords** Multiwalled carbon nanotubes · Polymers · Metal oxide · Supercapacitor stack · Asymmetry · Solid electrolyte

## Introduction

Supercapacitor can attain greater energy density than those of conventional capacitors and greater power density than batteries; this has kindled the interests of the researchers in this field of energy storage. As a result, supercapacitors may become an attractive power solution for an increasing number of applications. Electrical double layer capacitors (EDLCs) has the following advantages in energy storage system: long cycle life, high current capability, easily monitored state of charge, very high efficiency, wide voltage range, wide temperature range, long operational life, and ease of maintenance. Several attempts have been made to obtain fundamentally new materials and technologies for the design and manufacture of electrochemical supercapacitors. The present trend in research is focused on developing new supercapacitor electrode materials. Carbon nanotubes (CNTs) are materials with interesting properties such as increased accessible surface area, low mass density, and high electronic conductivity. These materials have then been studied by several authors in supercapacitor applications, mainly in aqueous electrolytes [1–5].

Transition metal oxides have been explored as potential electrode materials for use in supercapacitors; their charge-storage mechanisms are based predominantly on pseudocapacitance [6, 7]  $RuO_2$  has been found to have high capacitance due to redox transitions that even penetrates into the bulk of the material, however, the cost of Ru has retarded its commercial acceptance [8, 9]. Cheap metal oxides with comparable characteristics are being investigated, e.g., oxides of Ni, Co, In, Sn, Mn, etc and conducting polymers are another class of material under investigation due to their excellent electrochemical properties and low cost. Conducting polymer for redox supercapacitor has characteristic advantages, such as fast

---

A. Leela Mohana Reddy · F. Estaline Amitha · I. Jafri ·  
S. Ramaprabhu (✉)  
Alternative Energy Technology Laboratory, Department  
of Physics, Indian Institute of Technology Madras,  
Chennai 600 036, India  
e-mail: ramp@iitm.ac.in

kinetics of charge/discharge process and high charge storage capacitance [10]. The selection of Polyaniline (PANI) as electrode material for the supercapacitor is for the reason that it has good stability and reasonably priced [11–14].

An asymmetric configuration is obtained by using two different active materials as two electrodes. The asymmetric supercapacitor also improves power density by using high surface area nanostructured/nanofibrous electrode materials. It is demonstrated that a successful application of conducting polymers and metal oxides in supercapacitor technologies is possible only in an asymmetric configuration, i.e., with electrodes of different nature for positive and negative polarizations. Stacking of supercapacitors is desirable to produce devices that can operate at application voltages. By stacking two conventional double layer supercapacitor into a single component it is possible to get higher working voltage, thus enabling the use of supercapacitor for practical applications.

The objective of this work is to combine the advantages of the carbon nanotubes along with the transition metal oxide and polymer to fabricate the supercapacitor electrodes in asymmetric assembly. Further we have made use of the solid electrolyte to obtain all solid component supercapacitor with compact and flexible design. Two conventional supercapacitors are combined together to get a supercapacitor stack with a higher performance.

## Experiment

### Synthesis of Polymer and Metal Oxide MWNTs Nanocomposites

MWNTs were synthesized using a single stage furnace by thermal chemical vapor deposition (CVD) facility, by catalytic decomposition of acetylene over Mm based AB<sub>3</sub> alloy hydride catalysts. These catalysts were prepared through hydrogen decrepitation route by performing four cycles of hydrogenation/dehydrogenation of the alloy using a Seiverts apparatus [15] which causes plastic deformation in the lattice of the alloy and breaks them to fine particles. This alloy hydride powder was placed in quartz boat and kept at the center of a quartz tube, which was placed inside a tubular furnace. The quartz tube was maintained in argon atmosphere through out the process. Hydrogen was introduced into the quartz tube for 1 h at 500 °C. Further, the furnace was heated up to 700 °C followed by the introduction of acetylene for 30 min with a flow rate of 70 sccm. Then the furnace was cooled to room temperature. As-grown MWNTs samples were purified by air oxidation followed by refluxing with conc. nitric acid for 48 h [16]. The sample was washed with de-ionized water several times, filtered and dried at 80 °C for 2 h. Purified

MWNTs were ultrasonicated in conc. nitric acid for 3 h. Ultrasonication causes the formation of microbubbles which cause shock waves when they collapse and there by improves the nanotube wetting. After the sonication procedure, MWNT sample was refluxed under constant agitation in 30 mL of 70% HNO<sub>3</sub> at 110 °C for 12 h, followed by washing with deionized water several times and drying the sample in air for 30 min at 100 °C. These acid treated MWNT are thus called as functionalized MWNT.

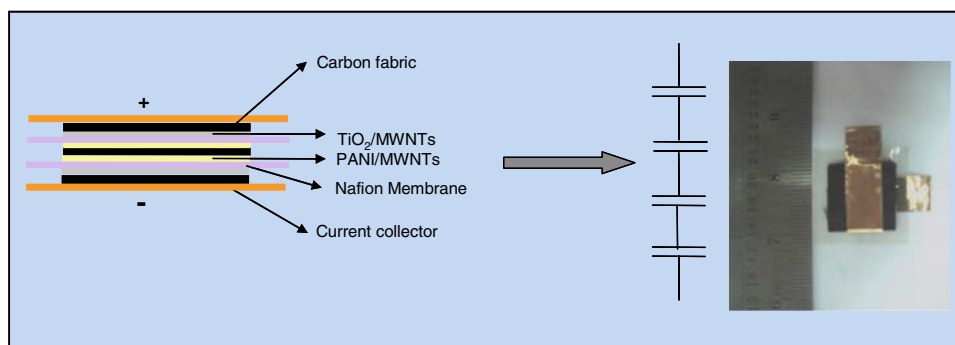
The PANI/MWNTs nanocomposite was synthesized via an in situ chemical oxidative polymerization method. 50 mL solution of 1.0 M HCl (37 wt%, Aldrich) containing 15 mg MWNTs was sonicated at room temperature for 2 days. 0.4 mL of aniline monomer was added to the above MWNTs suspension and sonicated for 6 h in icebath. 0.4 g of K<sub>2</sub>Cr<sub>2</sub>O<sub>7</sub> in 1.0 M HCl solution was then slowly added drop wise into the well-sonicated suspension with sonication at a reaction temperature of 0–5 °C for 30 min. The dark suspension became green, which indicated the beginning of polymerization reaction of aniline monomer. Then polymerization reaction was carried out at 0–5 °C for 24 h by putting the suspension into the refrigerator. The composites were obtained by filtering and rinsing the reaction mixtures several times with distilled water and methanol, resulting in the conductive emeraldine salt (ES) form of PANI/MWNTs composites. Finally, the dark-green composites powders were dried at 60 °C for 24 h under vacuum.

In case of TiO<sub>2</sub>/MWNTs preparation, functionalised MWNTs were first dispersed in dilute nitric acid (pH 0.5) by ultrasonic agitation. This solution is then transferred to a round bottom flask and titanium tetraisopropoxide was added drop wise maintaining the volume ratio of titanium tetraisopropoxide to water 1:4. The sol obtained was stirred for 2 days in air at room temperature. The obtained turbid suspension was centrifuged at 6000 rpm and the resultant residue was washed twice with distilled water. As synthesized TiO<sub>2</sub>/MWNT composites were heat treated at 350 °C for 2 h in air.

### Fabrication of Supercapacitor Stack

The 10 mg of PANI/MWNTs and TiO<sub>2</sub>/MWNTs each were taken and sonicated individually with few drops of de-ionized water and few drops of Nafion Solution for 10 min. This nanocomposite suspension was coated on flexible carbon fabric by spin coating. Three carbon fabric of 2.5 cm<sup>2</sup> each were taken, one of the carbon fabrics was coated with PANI/MWNTs on either sides and the other two carbon fabrics were coated on one side with TiO<sub>2</sub>/MWNTs. These are known as electrodes of supercapacitor. Nafion membrane is used as the solid electrolyte and the asymmetric supercapacitor stack assembly was obtained by

**Scheme 1** Schematic representation of supercapacitor stack



hot press, sandwiching two nafion membrane of  $3 \text{ cm}^2$  between the three electrodes as shown in Scheme 1 with a force of 1 Ton for 2 min at  $130^\circ\text{C}$ . The fabricated supercapacitor stack has been covered with two adhesive neoprene sheet of  $3 \text{ cm} \times 3 \text{ cm}$  size to obtain the complete supercapacitor. The idea of stacking supercapacitor is to obtain increase in voltage that could be applied to the supercapacitor. As the number of electrodes in the supercapacitor increases there is a cumulative result in the performance of the supercapacitor.

## Results and Discussion

MWNTs were synthesized by CVD using Mm based  $\text{AB}_3$  alloy hydride as catalyst prepared by hydrogenation and

dehydrogenation cycles. Figure 1a shows the XRD pattern of the as grown MWNTs with peaks corresponding to hexagonal graphite and catalytic impurities. Figure 1b shows the XRD pattern of purified sample which illustrates that the catalytic impurities have been efficiently removed

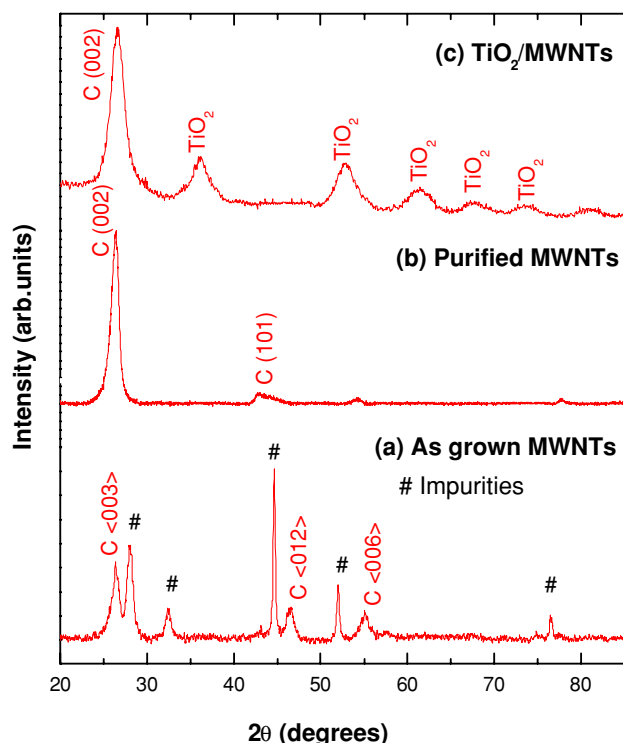


**Fig. 1** Powder X-ray diffractograms of (a) Grown MWNTs, (b) Purified MWNTs and (c)  $\text{TiO}_2/\text{MWNTs}$

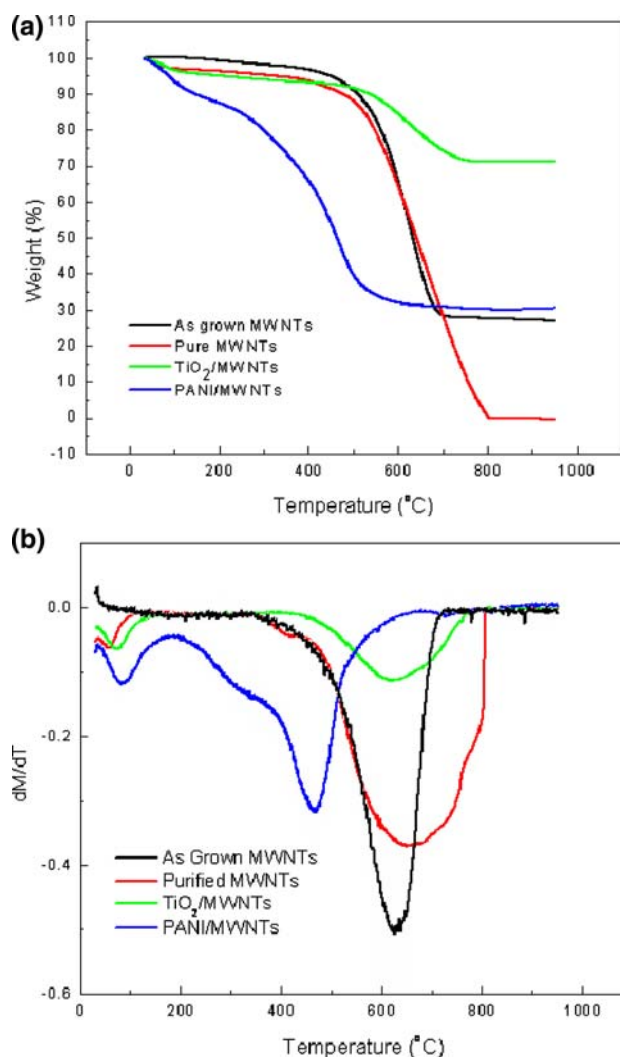


**Fig. 2** Thermogravimetry (TG) Curves of as grown MWNTs synthesized by the pyrolysis of acetylene over alloy hydride catalyst, Purified MWNTs,  $\text{TiO}_2/\text{MWNTs}$  and  $\text{PANI}/\text{MWNTs}$  (a) M versus T and (b)  $dM/dT$  versus T

during acid treatment [17]. The XRD pattern of  $\text{TiO}_2$ /MWNT nanocomposite material (Fig. 1c) shows the reflections of  $\text{TiO}_2$  along with that for graphitic carbon. The broad peaks of  $\text{TiO}_2$  reveal the presence of nano-structured metal oxide crystals.

Thermogravimetric measurements were performed using a STA 409PC TGA-DTA analyzer. The weight of the sample has been recorded as a function of temperature in the ranges of 25–950 °C. In the as grown sample the weight loss between 500 and 680 °C in the TG curves is attributed to the oxidation of MWNTs. Final residual weights of  $\sim 27\%$  were obtained for as grown MWNTs due to the presence of catalytic impurities. The weight loss between 500 and 800 °C in the purified sample is due to the oxidation of MWNTs and the residual weight is  $\sim 0\%$  revealing a purity of about  $\sim 98\%$  for the purified sample (Fig. 2a, b) [17]. The TGA of  $\text{TiO}_2$ /MWNTs shows weight loss between 500 and 750 °C which corresponds to oxidation of MWNTs and shows a residual weight of  $\sim 70\%$  which is due to the presence of  $\text{TiO}_2$  particles. The PANI/MWNTs shows weight loss from 200 °C which corresponds to the decomposition of polymer.

Figure 3 (a) SEM, (b) TEM and (c) HRTEM images confirm the good quality of the MWNTs obtained by CVD technique. The HRTEM image reveals the multi-walled nature of carbon nanotubes with each graphene layer being clearly distinguishable since the graphene sheets with a spacing of  $\sim 0.34$  nm are stacked parallel to the growth axis of carbon nanotubes. Figure 4(a, b) shows the SEM and TEM images of PANI/MWNTs composites which discloses the uniform dispersion of polymer over MWNTs surface. SEM and TEM images of  $\text{TiO}_2$ /MWNTs (Fig. 4(c, d)) indicate the uniform distribution of nano crystalline metal oxide particles of size of about 3–5 nm on the MWNTs.

The electrochemical properties of the flexible supercapacitor stack with solid electrolyte were studied. The cyclic voltammetry (CV) response of the super stack at scan rate  $0.1 \text{ Vs}^{-1}$  is shown in Fig. 5. There is a reasonable symmetry to the curves and the specific capacitance has been obtained from the CV curve according to following equation,

$$C_{\text{sp}} = i/[m * (dV/dt)] \quad (1)$$

where  $i$  is the average cathodic current,  $dV/dt$  is the potential sweep rate and  $m$  is the mass of each electrode.

**Fig. 3** (a) SEM, (b) TEM and (c) HRTEM images of purified MWNTs

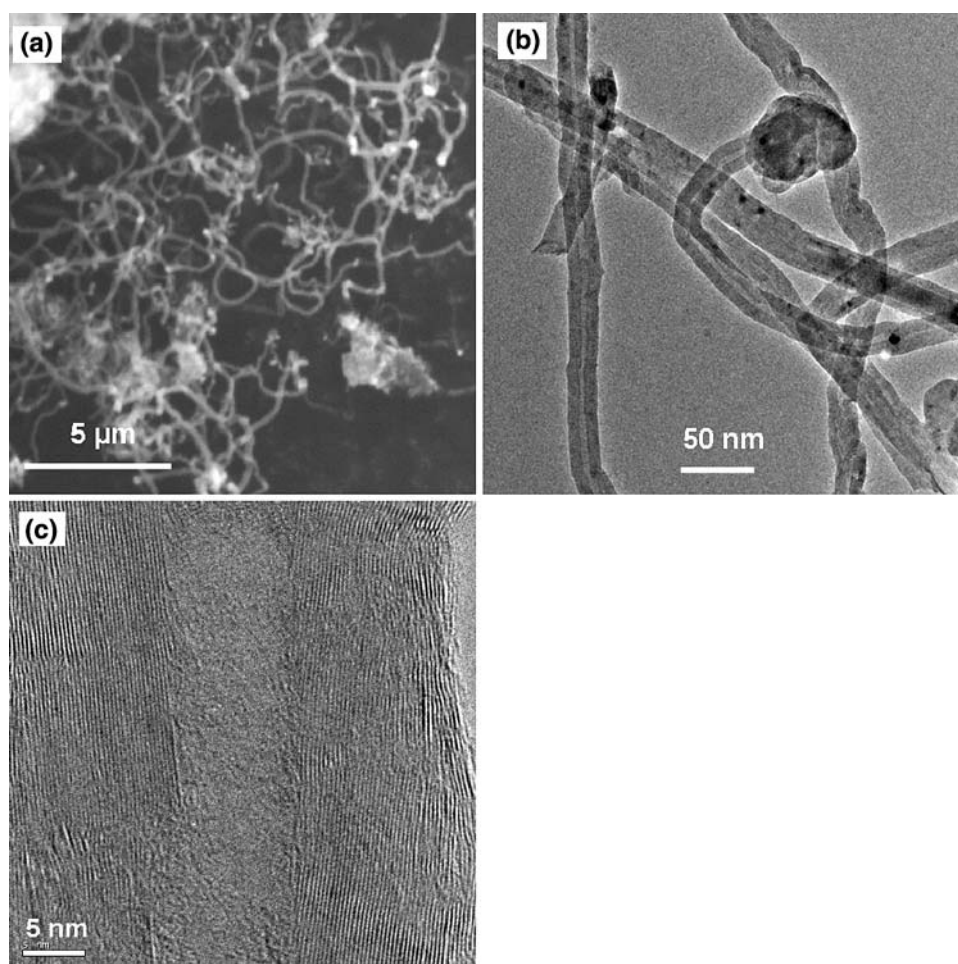




**Fig. 4** (a) SEM, (b) TEM images of PANI/MWNTs, (c) SEM and (d) TEM images of TiO<sub>2</sub>/MWNTs

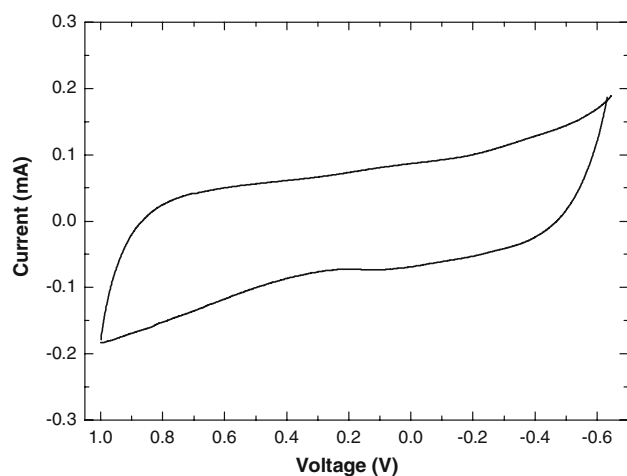
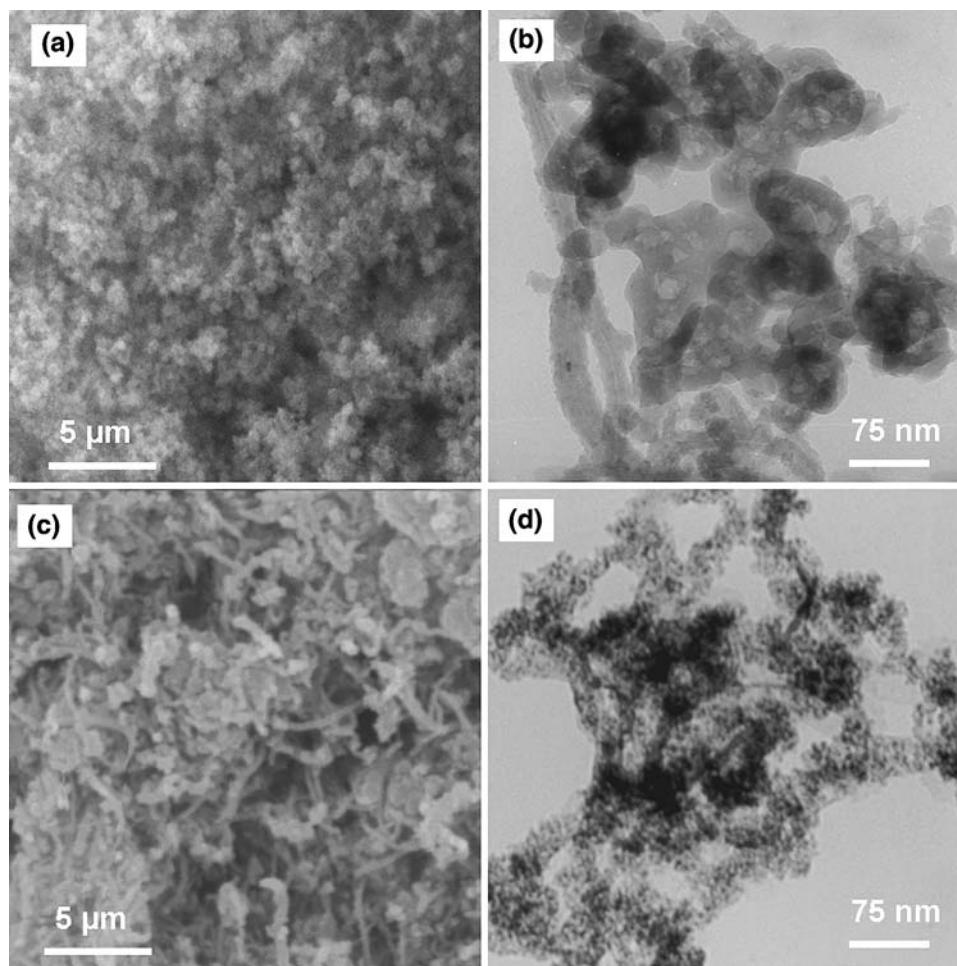


**Fig. 5** Cyclic voltammograms of asymmetric assembly of supercapacitor stack having PANI/MWNTs and TiO<sub>2</sub>/MWNTs as electrode materials at a scan rate of 2 mV s<sup>-1</sup>

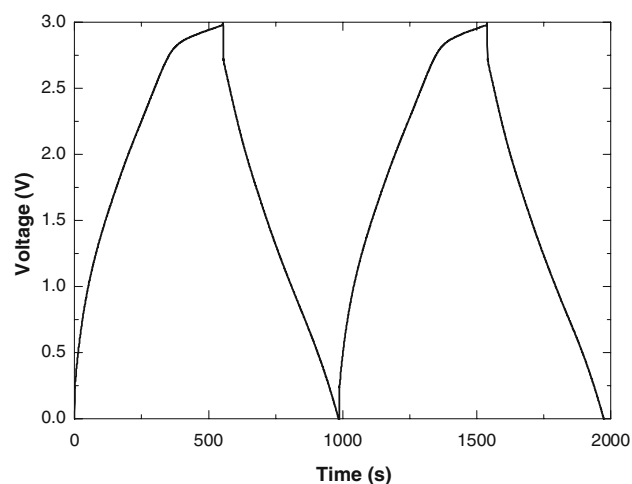


**Fig. 6** Galvanostatic charge discharge of asymmetric assembly of supercapacitor stack having PANI/MWNTs and TiO<sub>2</sub>/MWNTs as electrode materials at an applied constant current of 10 mA

Figure 6 shows the galvanostatic charge-discharge behavior of the supercapacitor stack with asymmetric assembly using PANI/MWNTs and TiO<sub>2</sub>/MWNTs with an

applied constant current of 10 mA in the potential range between 0 and +3 V. The symmetry of the charge and discharge characteristics shows good capacitive behavior.

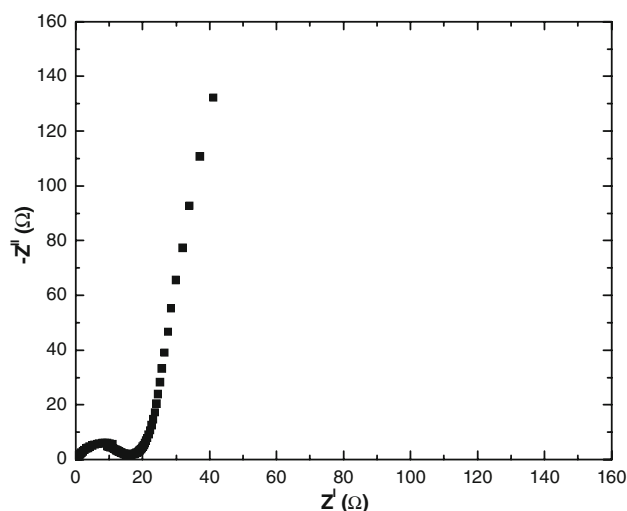


**Fig. 7** Complex-plane impedance spectra of asymmetric assembly of supercapacitor stack having PANI/MWNTs and  $\text{TiO}_2$ /MWNTs as electrode materials

The specific capacitance has been evaluated from the charge-discharge curves, according to the following equation:

$$C_{\text{sp}} = \frac{I}{m(dV/dt)} \quad (2)$$

where  $I$  is the applied current and  $m$  is the mass of each electrode.

Electrochemical Impedance Spectroscopy (EIS) measurements were carried out at a dc bias of 0 V with sinusoidal signal of 10 mV over the frequency range from 40 kHz to 10 MHz. Figure 7 presents complex-plane impedance plots for supercapacitor stack with PANI/MWNTs and  $\text{TiO}_2$ /MWNTs as the electrode materials with asymmetric assembly. At lower frequency, the imaginary part of impedance sharply increases: this is the capacitive behavior of electrode. The impedance plot should theoretically be a vertical line, parallel to the imaginary axis. In fact, the difference between this theoretical prediction and experiment can be observed. The impedance behavior of supercapacitor stack with PANI/MWNTs and  $\text{TiO}_2$ /MWNTs composites as electrodes show a deviation from ideal capacitor. The ac impedance method has also been used to measure the specific capacitance of the electrodes, which is influenced by the frequency, especially for porous electrodes, where almost no current flows down the pore at higher frequencies [18].

The average specific capacitances measured using the three electrochemical techniques of the supercapacitor stack with asymmetric assembly using polymer/MWNTs and metal oxide/MWNTs as electrodes and non-aqueous nafion membrane as electrolyte is 240 F/g. The capacitance values thus obtained here are comparatively more than

literature values (30 and 80 F/g for MWNTs,  $\text{RuO}_2$ /MWNTs, respectively) [19]. The capacitance of the MWNTs is mainly due to several factors including (1) a homogeneous inter-distribution of carbon/Nafion in electrodes, (2) an excellent adhesion realized between electrodes and Nafion membrane, (3) a good contact between electrodes and end plates, (4) fast proton transport in smaller carbon pores. Further uniform dispersion of polymer and metal oxide particles over functionalized MWNTs also contributes to the increase in the capacitance. Since the specific double layer capacitance arises from the ionic double layer at the electrode/electrolyte interface, the accessibility of the active layer depends on the diffusion of solvated ions and more precisely on the pore size distribution. The central hollow core of the CNTs is also accessible for the double layer charging and thus the purified MWNTs with opened tips along with the unique network of mesopores formed by the entanglement of CNTs would have acted as sites for the accumulation of charges. The enhancement of the specific capacitances can be attributed to the presence of polymer and metal oxide attached to the surface of MWNTs, which in turn modify the microstructure and morphology of MWNTs, allowing the polymer and metal oxides to be available for the electrochemical reactions and improves the efficiency of the composites. The progressive redox reactions occurring at the surface and bulk of polymer and metal oxides through faradiac charge transfer between electrolyte and electrode results in the enhancement of the specific capacitance of polymer and metal oxide dispersed MWNTs from pure MWNTs.

## Conclusions

A non-aqueous electrolyte based supercapacitor stack has been fabricated successfully using asymmetric combination of PANI/MWNTs and  $\text{TiO}_2$ /MWNTs coated flexible electrode materials. A maximum specific capacitance of 240 F/g has been derived from the supercapacitor stack.

**Acknowledgments** We thank MHRD, NRB and DRDO, Govt. of India, for the financial support of this work.

## References

1. F. Frackowiak, K. Jurewicz, K. Szostak, S. Delpeux, F. Beguin, *Fuel Process. Technol.* **213**, 77 (2002)
2. B.-J. Yoon, S.-H. Jeong, K.-H. Lee, H.S. Kim, C.G. Park, J.H. Han, *Chem. Phys. Lett.* **388**, 170 (2004)
3. A.K. Chatterjee, M. Sharon, R. Banerjee, M. Neumann-Spallart, *Electrochem. Acta* **48**, 3439 (2003)
4. Ch. Emmenegger, P. Mauron, A. Züttel, Ch. Niitzenadel, A. Schneuwly, R. Gallay, L. Schlapbach, *Appl. Surf. Sci.* **162–163**, 452 (2000)

5. J.H. Chen, W.Z. Li, D.Z. Wang, S.X. Yang, J.G. Wen, Z.F. Ren, *Carbon* **40**, 1193 (2002)
6. M. Toupin, T. Brousse, D. Belanger, *Chem. Mater.* **16**, 3184 (2004)
7. M. Toupin, T. Brousse, D. Belanger, *Chem. Mater.* **14**, 3946 (2002)
8. H. Kim, B.N. Popov, *J. Power Sour.* **104**, 52 (2002)
9. J.P. Zheng, P.J. Cyjan, T.R. Jow, *J. Electrochem. Soc.* **142**, 2699 (1995)
10. C. Arbizzani, M. Mastragostino, B. Scrosati, in *Handbook of Organic Conductive Molecules and Polymers*, ed. by B.H.S. Nalwa (John Wiley & Sons, 1997), Chapter 11
11. K. Rajendra Prasad, N. Munichandraiah, *J. Power Sour.* **112**, 443 (2002)
12. A. Burke, *J. Power Sour.* **91**, 37 (2000)
13. B.E. Conway, *Electrochemical Supercapacitors: Scientific Fundamentals and Technological Applications* (Kluwer Academic, Plenum Publishers, New York, 1999), Chapter 2
14. G. Gottesfeld, A. Redondo, S.W. Feldberg, *J. Electrochem. Soc.* **134**, 271 (1987)
15. M.M. Shaijumon, N. Rajalakshmi, H. Ryu, S. Ramaprabhu, *Nanotechnology* **16**, 518 (2005)
16. A.G. Rinzler, J. Liu, H. Dai, P. Nikolaev, C.B. Huffman, F.J. Rodriguez-Macias, P.J. Boul, A.H. Lu, D. Heymann, D.T. Colbert, R.S. Lee, J.E. Fischer, A.M. Rao, P.C. Eklund, R.E. Smalley, *Appl. Phys. A* **67**, 29 (1998)
17. F. Estaline Amitha, A. Leela Mohana Reddy, S. Ramaprabhu, *J. Nanopart. Res.* (Accepted for publication 2008)
18. R. Kötz, M. Carlen, *Electrochim. Acta.* **45**, 2483 (2000)
19. G. Arabale, D. Wagh, M. Kulkarni, I.S. Mulla, S.P. Vernekar, K. Vijayamohanan, A.M. Rao, *Chem. Phys. Lett.* **376**, 207 (2003)